1:2000; anti-pS422, 1:1000; or anti–α-tubulin, 1:10,000) (Table 1) overnight at room temperature. For phosphor-(Ser/Thr) kinase substrate assay, phospho-(Thr) mitogen-activated protein kinase/cyclin-dependent kinase (MAPK/CDK) substrate mouse monoclonal antibody (1:1000), phosphor-Akt substrate rabbit monoclonal antibody (1:1000), phosphor–protein kinase A (PKA) substrate rabbit monoclonal antibody (1:1000), phosphor–(Ser) protein kinase C (PKC) substrate rabbit polyclonal antibody (1:1000), and phosphor-(Ser) CDKs substrate rabbit polyclonal antibody (1:1000), which were obtained from Cell Signaling Technology, Inc (Danvers, MA), were used (Table 1). After incubation with a secondary antibody (1:50,000; Bio-Rad), immunoreactivity was detected by the chemiluminescence method using an ECL plus Western Blotting Detection Kit (GE Healthcare UK Ltd, Buckinghamshire, UK) or Super Signal West Dura (Thermo Scientific, West Palm Beach, FL) and was visualized with LAS-4000 mini (GE Healthcare UK Ltd). For quantitative measure of band intensity, α-tubulin was used as an internal control for protein concentration.

Analysis of Tau Deposition

For fluorescent immunohistochemistry, sagittal sections were cut serially on a freezing microtome at 30-μm thickness, collected in the maintenance solution, and immunostained as free-floating sections. Sections were incubated for 24 hours with anti-pS422 antibody (1:500; Dr Hasegawa). The antibody labeling was visualized by incubation with Alexa Fluor 488–conjugated goat anti-rabbit IgG (1:100; Invitrogen, Carlsbad, CA) for 3 hours. The sections were then rinsed with distilled water, mounted on glass slides, coverslipped with ProLong Gold Antifade Reagent (Invitrogen). Photographs were taken with a BioZero (Keyence, Osaka, Japan). The fluorescent positive cells were counted in the area of 820 × 1,080 μm of the external cortex of the inferior colliculus.

Statistical Analyses

Data are presented as mean ± SE. The statistical significance of differences in the mean values between 2 populations was assessed with the Student *t*-test, whether

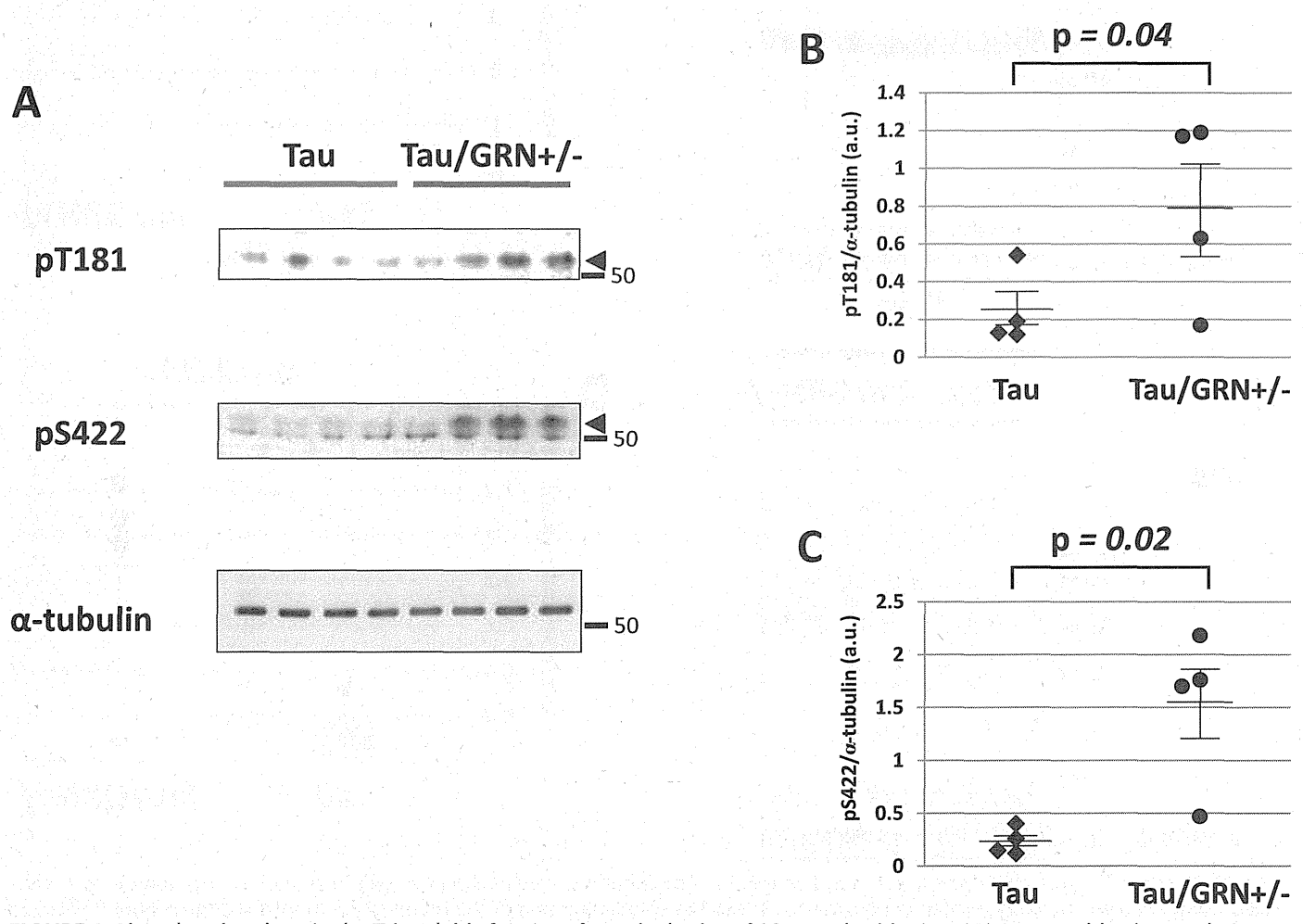

FIGURE 2. Phosphorylated tau in the Tris-soluble fractions from the brains of 13-month-old mice. **(A)** Immunoblotting analysis was visualized using pT181 and pS422 and antibodies for detecting phosphorylated tau in Tris-soluble fraction of 13-month-old mice. Black arrowhead indicates phosphorylated tau. **(B, C)** A comparison of relative phosphorylated tau (**[B]** pT181, **[C]** pS422) expression levels. Data were compared with the band median intensity/α-tubulin. $p < 0.05$ was considered significant by Student *t*-test **(B)** and Mann-Whitney U test **(C)**. a.u., arbitrary units. The loading control (α-tubulin) is also shown. Molecular weight markers are shown on the right (kDa).

variances were equal was determined by an F-test, and otherwise we used the Mann-Whitney U test. $p < 0.05$ was considered significant.

RESULTS

Phosphorylated Tau in the Tris-Soluble Fraction of 13-Month-Old Tau/*GRN*$^{+/-}$ Mice

Brains were collected from 13-month-old mice of P301L tau or P301L tau/*GRN*$^{+/-}$, and sequential protein extraction and immunoblotting were performed. On immunoblotting, total tau was detected by phosphorylation-independent anti-tau antibody, T46 (Fig. 1A, B); phosphorylated tau was revealed by phosphorylation-dependent anti-tau antibodies, including AT8 (Fig. 1C, D), pT181, and pS422 (Fig. 2A–C). The amount of total tau in the Tris-soluble fraction was almost the same in both mouse strains (Fig. 1A, B). On the other hand, the amounts of phosphorylated tau in the Tris-soluble fractions detected by AT8 (Fig. 1C, D), pT181 (Fig. 2A, B), and pS422 (Fig. 2A, C) were significantly higher in P301L tau/*GRN*$^{+/-}$ mice than in P301L tau mice. The AT8/α-tubulin ratio was 0.09 ± 0.06 (n = 4) in the P301L tau mice and 1.02 ± 0.25 (n = 4) in the P301L tau/*GRN*$^{+/-}$ mice (Fig. 1D). The Mann-Whitney U test was used for statistical analysis, and there was a significant difference between the P301L tau mice and the P301L tau/*GRN*$^{+/-}$ mice ($F = 0.047$, $p = 0.03$). The pT181/α-tubulin ratio was 0.16 ± 0.10 (n = 4) in the P301L tau mice and 0.90 ± 0.25 (n = 4) in the P301L tau/*GRN*$^{+/-}$ mice (Fig. 2B). There was a significant difference between the P301L tau mice and the P301L tau/*GRN*$^{+/-}$ mice ($F = 0.172$, $p = 0.04$). The pS422/α-tubulin ratio was 0.20 ± 0.06 (n = 4) in the P301L tau mice and 1.73 ± 0.37 (n = 4) in the P301L tau/*GRN*$^{+/-}$ mice (Fig. 2C). There was a significant difference between the P301L tau mice and the P301L tau/*GRN*$^{+/-}$ mice ($F = 0.016$, $p = 0.02$). Phosphorylated tau was not detected in the sarkosyl-insoluble fraction in either mouse strain (data not shown).

Phosphorylated Tau in the Sarkosyl-Insoluble Fraction of 19-Month-Old P301L Tau/*GRN*$^{+/-}$ Mice

Brains were collected from 19-month-old mice of P301L tau or P301L tau/*GRN*$^{+/-}$, and sequential protein extraction and immunoblotting were performed. Phosphorylated tau in the sarkosyl-insoluble fraction was visualized by

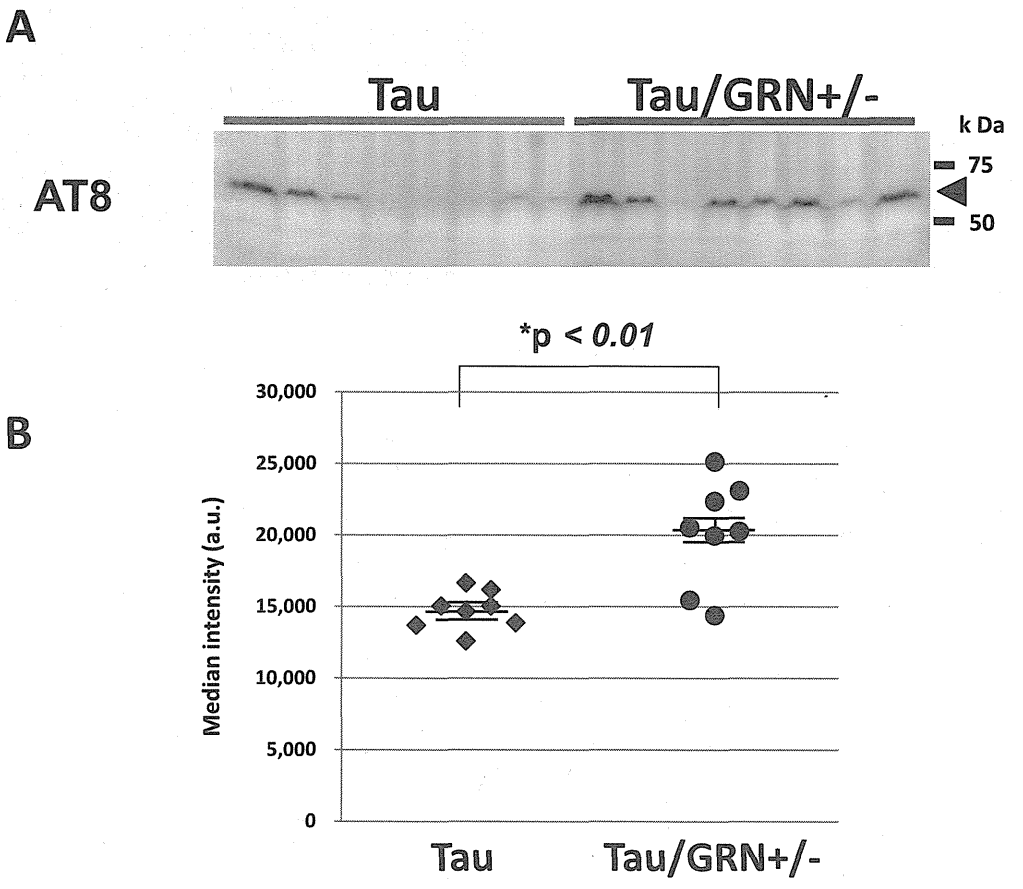

FIGURE 3. Immunoblotting analysis of phosphorylated tau in sarkosyl-insoluble fractions from the brains of 19-month-old mice. **(A)** Immunoblotting analysis was visualized using the AT8 antibody for detecting phosphorylated tau in sarkosyl-insoluble fractions from brains of 19-month-old mice. Black arrowhead indicates phosphorylated tau. Molecular weight markers are shown on the right (kDa). **(B)** A comparison of relative phosphorylated tau (AT8) expression levels in the sarkosyl-insoluble fractions. Data were compared with the AT8 band median intensity. $p < 0.05$ was considered to significant by Mann-Whitney U test. a.u., arbitrary units.

Western blotting using the AT8 antibody (Fig. 3A). The median intensities were significantly higher in the P301L tau/*GRN*$^{+/-}$ mice (20,156.3 ± 1,296.5, n = 8) than in the P301L tau mice (14,720.4 ± 470.1, n = 8) (Fig. 3B). These results suggest that the level of abnormally phosphorylated tau accumulation was increased in the P301L tau/*GRN*$^{+/-}$ mice as compared with the P301L tau mice.

Phosphorylated Tau in 19-Month-Old Mice by Immunofluorescence Staining

Phosphorylated tau in the area of the external cortex of the inferior colliculus of 19-month-old P301L tau and P301L tau/*GRN*$^{+/-}$ was visualized using immunofluorescence staining with an anti-pS422 antibody (Fig. 4). The pS422-positive cells were increased in P301L tau/*GRN*$^{+/-}$ mice (289 ± 43 cells, n = 3) compared with P301L tau mice (94 ± 23 cells, n = 3) (F = 3.528, p = 0.03 by Student *t*-test).

Kinase Activity Using Phosphor-(Ser/Thr) Kinase Substrate Antibodies

Determining kinase activities in the brains of P301L tau and P301L tau/*GRN*$^{+/-}$ mice by immunoblotting was performed using phosphor-(Ser/Thr) kinase substrate antibodies. There were no differences detected for phospho-(Thr) MAPK/CDK substrate, phospho-Akt substrate, phospho-PKA substrate, and phosphor-(Ser) PKC substrate in Tris-soluble fractions of 13-month-old P301L tau and P301L tau/*GRN*$^{+/-}$ mice (Fig. 5A–D). By contrast, the phospho-(Ser) CDK substrate was more prominently phosphorylated in P301L tau/*GRN*$^{+/-}$ mice than in the P301L tau mice (Fig. 5E). The approximately 60-kDa band/α-tubulin ratio was 2.04 ± 0.22 (n = 4) in the P301L tau mice and 3.08 ± 0.39 (n = 4) in the P301L tau/*GRN*$^{+/-}$ mice (Figure, part A, Supplemental Digital Content 1, http://links.lww.com/NEN/A697). There was a significant difference between the P301L tau mice and the P301L tau/*GRN*$^{+/-}$ mice (F = 0.358, p = 0.03; Figure, part B, Supplemental Digital Content 1, http://links.lww.com/NEN/A697) (Student *t*-test).

DISCUSSION

The results of the present study show that *GRN* mutations causing PGRN reduction are associated with increased phosphorylation and intracellular accumulation of tau in mice harboring the P301L tau mutation. They suggest that *GRN* mutations causing PGRN reduction may be causative or risk factors for tauopathies. Indeed, there are many reports of *GRN* mutations associated with AD (Table 2). Furthermore, in a large Belgian FTLD pedigree with a *GRN* ISV1+5G > C mutation, a few patients had a cerebrospinal fluid biomarker profile typical of AD, that is, decreased amyloid-β protein (1–42) and increased total tau and phosphorylated tau (p181) (12). Another patient in the pedigree had comorbidity of FTLD-TDP and dementia with Lewy bodies with AD pathology at autopsy.

In this study, we showed accelerated phosphorylation of tau in Tris-soluble and sarkosyl-insoluble fractions in P301L tau/*GRN*$^{+/-}$ mice compared with P301L tau mice. To identify the responsible kinases, we performed immunoblotting analysis using phosphor-(Ser/Thr) kinase substrate antibodies.

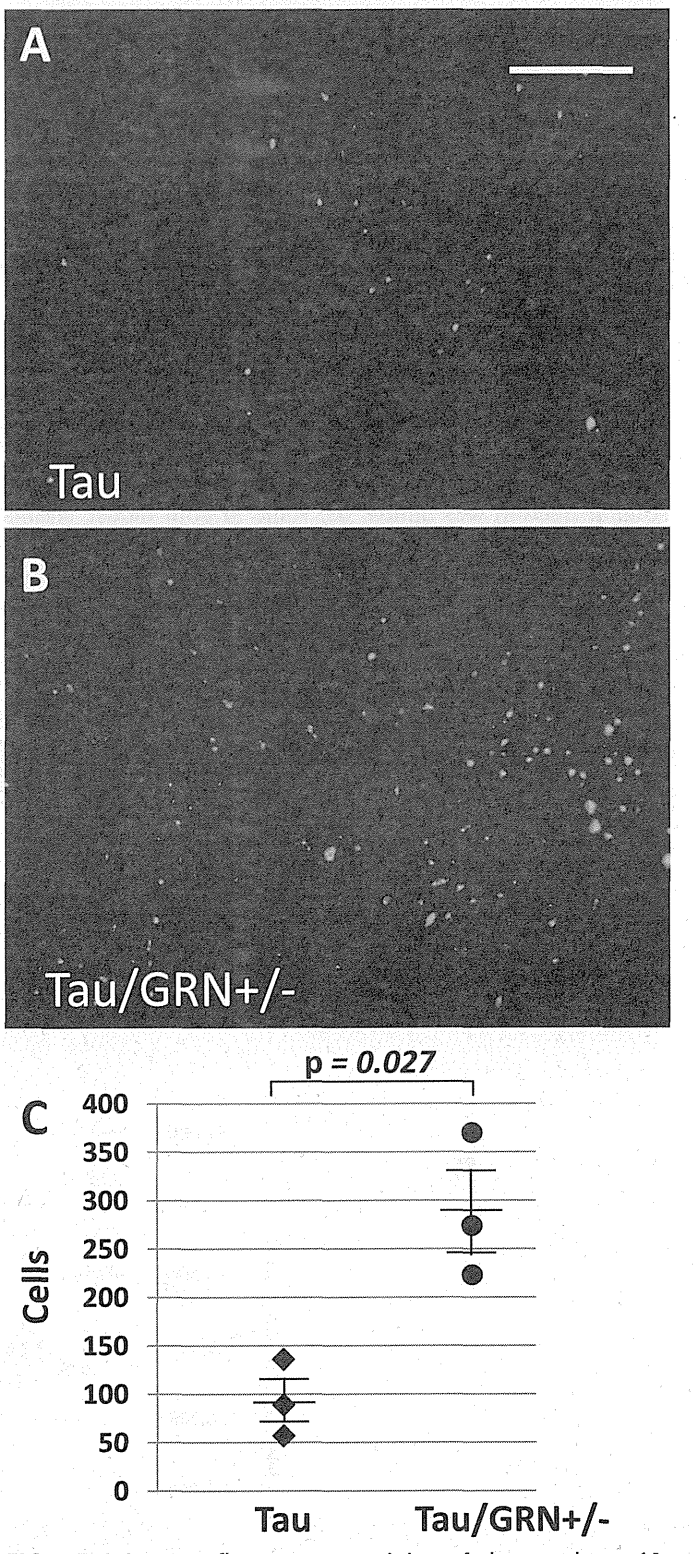

FIGURE 4. Immunofluorescence staining of abnormal tau. **(A, B)** pS422 immunoreactivity was observed in the midbrain of P301L tau mice **(A)** and P301L tau/GRN$^{+/-}$ mice **(B)**. The calibration bar in **(A)** applies to both panels (200 μm). **(C)** Comparison of pS422-positive cell numbers in the 2 sets of mice. The data were compared with the pS422-positive cell numbers in the external cortex of the inferior colliculus. $p < 0.05$ was considered significant by Student *t*-test.

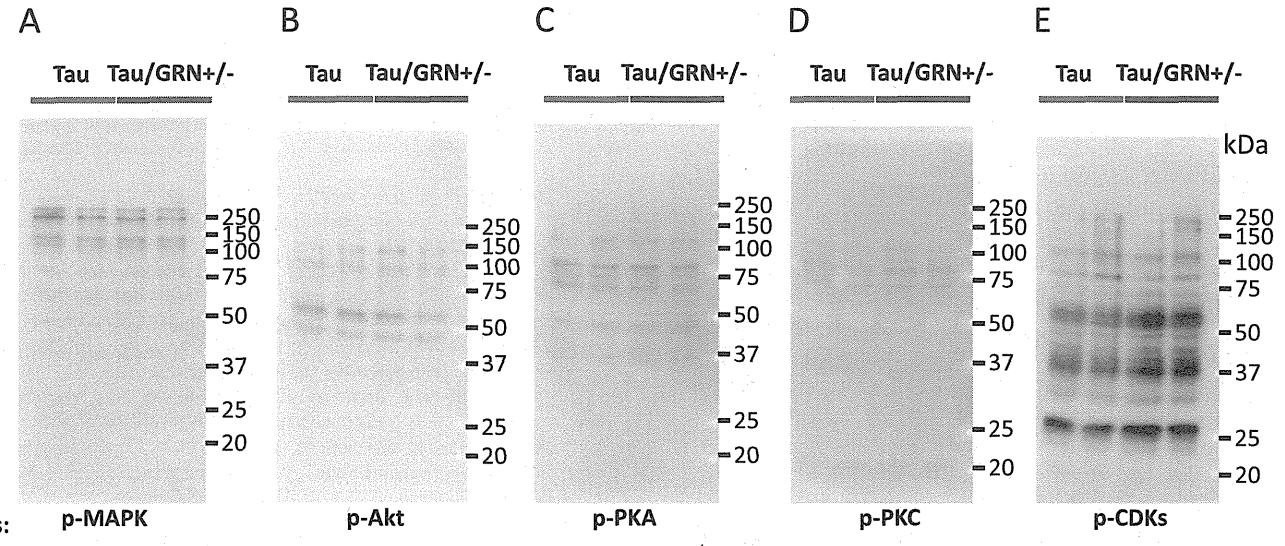

FIGURE 5. Kinase activities in the brains of 13-month-old P301L tau/GRN$^{+/-}$ and P301L tau mice. **(A–E)** Kinase activities in the brains were visualized using phosphor-(Ser/Thr) kinase substrate antibodies as follows: phosphor-MAPK, mitogen-activated protein kinase (p-MAPK) substrate antibody **(A)**, phosphor-Akt substrate antibody (p-AKT) **(B)**, phosphor-protein kinase A (p-PKA) substrate antibody **(C)**, phosphor-protein kinase C (p-PKC) substrate antibody **(D)**, and p-cyclin–dependent kinases (CDKs) substrate antibody **(E)**. Molecular weight markers are shown on the right (kDa).

Strong phosphorylation of CDK substrates observed in P301L tau/*GRN*$^{+/-}$ mice brain compared with P301L tau mice suggests that CDKs might be activated by *GRN* deficiency resulting in increased phosphorylated tau (Fig. 5E). There were no significant differences of phosphorylation levels in substrates for MAPK, Akt, PKA, or PKC (Fig. 5A–D). Furthermore, there were no significant differences in the amount of the phosphorylated GSK-3β in the Tris-soluble fraction between P301L tau/*GRN*$^{+/-}$ mice and P301L tau mice (data not shown). These results suggest that these kinases were not involved in the accelerated phosphorylation of tau in P301L tau/*GRN*$^{+/-}$ mice.

The mechanisms by which *GRN* hemi-knockout may activate CDKs and accelerate tau pathology in P301L tau mice are not known and require future exploration. The proinflammatory effects of PGRN downregulation might also accelerate abnormal tau phosphorylation. There is a report

TABLE 2. *GRN* Mutations That Have Been Confirmed in Patients Clinically Diagnosed as Having Alzheimer Disease

Putative Loss-of-Function Mechanism	Mutation (Gene)	Mutation (Protein)	Clinical Phenotype	Reference
Loss of DNA	IVS0+5G > C	p.0	AD, PD	(12)
Loss of transcript	IVS1+5G > C	p.0	AD, FTD, PA	(16)
	c.154delA	pT52HfsX2	AD, FTD	(14)
	c.361delG	p.V121WfsX135	AD	(13)
	c.388_391delCAGT	p.Q130SfsX125	AD	(18)
	c.463_598del	p.A155WfsX56	AD	(13)
	c.592_593delAG	p.R198GfsX19	AD	(17)
	c.813_816delCACT	p.T272SfsX10	AD	(13)
	c.1477C > T	p.R493X	AD, FTD	(14)
	c.1603C > T	p.R535X	AD	(12)
Loss of protein function	c.103G > A	p.G35R	AD	(20)
	c.415 T > C	p.C139R	AD, PA, FTD	(17, 19)
	c.1352C > T	p.P451L	AD	(19)
	c.1690C > T	p.R564C	AD	(19)
Unknown pathogenic nature	c.99C > A	p.D33E	AD	(19)
	c.781C > T	p.L261I	AD	(19)
	c.970G > A	p.A324T	AD, PA	(17, 19)
	c.1297C > T	p.R433W	AD, PA, SD	(17, 19)
	c.1540G > A	p.V514M	AD	(19)
	c.1544G > C	p.G515A	AD	(19)
	3'UTR +78C > T	(rs5848)	AD	(22, 23)

AD, Alzheimer disease; CBS, corticobasal syndrome; FTD, frontotemporal dementia; FTLD, frontotemporal lobar degeneration; PA, progressive nonfluent aphasia; PD, Parkinson disease ; p.0, progranulin null.

that PGRN binds to tumor necrosis factor receptors and prevents inflammation (32). Recently, a number of studies with tau transgenic mice have shown that inflammation exacerbates tau pathology in these mice (33–35). In the present study, we measured expression levels of inflammatory cytokines (interleukin 1β) or cyclooxygenase-2, but they were not increased in P301L tau/*GRN*$^{+/-}$ mice (data not shown).

The mechanism of CDK activation and accumulation of phosphorylated tau caused by PRGN deficiency should be investigated further, but the results of the present study suggest that *GRN* mutations might contribute to the pathogenesis or be risk factors for tauopathies, including AD. Controlling PGRN levels or suppressing CDK activation may be useful therapy in tauopathy cases with *GRN* mutations.

ACKNOWLEDGMENTS

The authors thank Drs Takashi Nonaka and Makiko Yamashita for helpful comments and Ms Erika Arakawa for technical assistance and animal care. The authors thank Dr Edith G. McGeer for editing of the manuscript.

REFERENCES

1. Daniel R, Daniels E, He Z, et al. Progranulin (acrogranin/PC cell–derived growth factor/granulin-epithelin precursor) is expressed in the placenta, epidermis, microvasculature, and brain during murine development. Dev Dyn 2003;227:593–99
2. Van Damme P, Van Hoecke A, Lambrechts D, et al. Progranulin functions as a neurotrophic factor to regulate neurite outgrowth and enhance neuronal survival. J Cell Biol 2008;181:37–41
3. He Z, Ong CH, Halper J, et al. Progranulin is a mediator of the wound response. Nat Med 2003;9:225–29
4. Zhu J, Nathan C, Jin W, et al. Conversion of proepithelin to epithelins: Roles of SLPI and elastase in host defense and wound repair. Cell 2002; 111:867–78
5. Yin F, Banerjee R, Thomas B, et al. Exaggerated inflammation, impaired host defense, and neuropathology in progranulin-deficient mice. J Exp Med 2010;207:117–28
6. Ong CH, Bateman A. Progranulin (granulin-epithelin precursor, PC-cell derived growth factor, acrogranin) in proliferation and tumorigenesis. Histol Histopathol 2003;18:1275–88
7. Pickford F, Marcus J, Camargo LM, et al. Progranulin is a chemoattractant for microglia and stimulates their endocytic activity. Am J Pathol 2011; 178:284–95
8. Baker M, Mackenzie IR, Pickering-Brown SM, et al. Mutations in progranulin cause tau-negative frontotemporal dementia linked to chromosome 17. Nature 2006;442:916–19
9. Cruts M, Gijselinck I, van der Zee J, et al. Null mutations in progranulin cause ubiquitin-positive frontotemporal dementia linked to chromosome 17q21. Nature 2006;442:920–24
10. Gass J, Cannon A, Mackenzie IR, et al. Mutations in progranulin are a major cause of ubiquitin-positive frontotemporal lobar degeneration. Hum Mol Genet 2006;15:2988–3001
11. Mukherjee O, Pastor P, Cairns NJ, et al. HDDD2 is a familial frontotemporal lobar degeneration with ubiquitin-positive, tau-negative inclusions caused by a missense mutation in the signal peptide of progranulin. Ann Neurol 2006;60:314–22
12. Brouwers N, Nuytemans K, van der Zee J, et al. Alzheimer and Parkinson diagnoses in progranulin null mutation carriers in an extended founder family. Arch Neurol 2007;64:1436–46
13. Le Ber I, Camuzat A, Hannequin D, et al. Phenotype variability in progranulin mutation carriers: A clinical, neuropsychological, imaging and genetic study. Brain 2008;131:732–46
14. Kelley BJ, Haidar W, Boeve BF, et al. Prominent phenotypic variability associated with mutations in progranulin. Neurobiol Aging 2009;30: 739–51
15. Rademakers R, Baker M, Gass J, et al. Phenotypic variability associated with progranulin haploinsufficiency in patients with the common 1477C–> T (Arg493X) mutation: An international initiative. Lancet Neurol 2007;6: 857–68
16. Sleegers K, Brouwers N, Van Damme P, et al. Serum biomarker for progranulin-associated frontotemporal lobar degeneration. Ann Neurol 2009;65:603–9
17. Finch N, Baker M, Crook R, et al. Plasma progranulin levels predict progranulin mutation status in frontotemporal dementia patients and asymptomatic family members. Brain 2009;132:583–91
18. Carecchio M, Fenoglio C, De Riz M, et al. Progranulin plasma levels as potential biomarker for the identification of GRN deletion carriers. A case with atypical onset as clinical amnestic mild cognitive impairment converted to Alzheimer's disease. J Neurol Sci 2009;287:291–93
19. Brouwers N, Sleegers K, Engelborghs S, et al. Genetic variability in progranulin contributes to risk for clinically diagnosed Alzheimer disease. Neurology 2008;71:656–64
20. Cortini F, Fenoglio C, Guidi I, et al. Novel exon 1 progranulin gene variant in Alzheimer's disease. Eur J Neurol 2008;15:1111–17
21. Kelley BJ, Haidar W, Boeve BF, et al. Alzheimer disease-like phenotype associated with the c.154delA mutation in progranulin. Arch Neurol 2010;67:171–77
22. Fenoglio C, Galimberti D, Cortini F, et al. Rs5848 variant influences GRN mRNA levels in brain and peripheral mononuclear cells in patients with Alzheimer's disease. J Alzheimers Dis 2009;18:603–12
23. Lee MJ, Chen TF, Cheng TW, et al. rs5848 variant of progranulin gene is a risk of Alzheimer's disease in the Taiwanese population. Neurodegener Dis 2011;8:216–20
24. Perry DC, Lehmann M, Yokoyama JS, et al. Progranulin mutations as risk factors for Alzheimer disease. JAMA Neurol 2013;70:774–78
25. Masellis M, Momeni P, Meschino W, et al. Novel splicing mutation in the progranulin gene causing familial corticobasal syndrome. Brain 2006; 129:3115–23
26. Benussi L, Binetti G, Sina E, et al. A novel deletion in progranulin gene is associated with FTDP-17 and CBS. Neurobiol Aging 2008;29:427–35
27. Spina S, Murrell JR, Huey ED, et al. Corticobasal syndrome associated with the A9D Progranulin mutation. J Neuropathol Exp Neurol 2007;66: 892–900
28. Leverenz JB, Yu CE, Montine TJ, et al. A novel progranulin mutation associated with variable clinical presentation and tau, TDP43 and alpha-synuclein pathology. Brain 2007;130:1360–74
29. Lewis J, McGowan E, Rockwood J, et al. Neurofibrillary tangles, amyotrophy and progressive motor disturbance in mice expressing mutant (P301L) tau protein. Nat Genet 2000;25:402–5
30. Kayasuga Y, Chiba S, Suzuki M, et al. Alteration of behavioural phenotype in mice by targeted disruption of the progranulin gene. Behav Brain Res 2007;185:110–18
31. Greenberg SG, Davies P. A preparation of Alzheimer paired helical filaments that displays distinct tau proteins by polyacrylamide gel electrophoresis. Proc Natl Acad Sci U S A 1990;87:5827–31
32. Tang W, Lu Y, Tian QY, et al. The growth factor progranulin binds to TNF receptors and is therapeutic against inflammatory arthritis in mice. Science 2011;332:478–84
33. Kitazawa M, Oddo S, Yamasaki TR, et al. Lipopolysaccharide-induced inflammation exacerbates tau pathology by a cyclin-dependent kinase 5-mediated pathway in a transgenic model of Alzheimer's disease. J Neurosci 2005;25:8843–53
34. Lee DC, Rizer J, Selenica ML, et al. LPS-induced inflammation exacerbates phospho-tau pathology in rTg4510 mice. J Neuroinflammation 2010;7:56
35. Sy M, Kitazawa M, Medeiros R, et al. Inflammation induced by infection potentiates tau pathological features in transgenic mice. Am J Pathol 2011;178:2811–22

NEUROPATHOLOGY

Neuropathology 2014; **34**, 578–588 doi:10.1111/neup.12138

Symposium: Definition and Differentials – How to Distinguish Disease-Specific Changes on Microscopy

Significance and limitation of the pathological classification of TDP-43 proteinopathy

Tetsuaki Arai[1,2]

[1]Department of Neuropsychiatry, Division of Clinical Medicine, Faculty of Medicine, University of Tsukuba, Tsukuba and [2]Department of Dementia and Higher Brain Function, Tokyo Metropolitan Institute of Medical Science, Tokyo, Japan

Based on the cerebral tans-activation response DNA protein 43 (TDP-43) immunohistochemistry, frontotemporal lobar degeneration with TDP-43 pathology (FTLD-TDP) is classified into four subtypes: type A has numerous neuronal cytoplasmic inclusions (NCIs) and dystrophic neurites (DNs); type B has numerous NCIs with few DNs; type C is characterized by DNs which are often longer and thicker than DNs in type A, with few NCIs; and type D has numerous neuronal intranuclear inclusions and DNs with few NCIs. The relevance of this classification system is supported by clinical, biochemical and genetic correlations, although there is still significant heterogeneity, especially in cases with type A pathology. The subtypes of TDP-43 pathology should be determined in cases with other neurodegenerative disorders, including Alzheimer's disease and dementia with Lewy bodies, to evaluate the pathological significance of TDP-43 abnormality in them. The results of the biochemical analyses of the diseased brains and the cellular models suggest that different strains of TDP-43 with different conformations may determine the clinicopathological phenotypes of TDP-43 proteinopathy, like prion disease. Clarifying the mechanism of the conformational changes of TDP-43 leading to the formation of multiple abnormal strains may be important for differential diagnosis and developing disease-modifying therapy for TDP-43 proteinopathy.

Key words: fragment, phosphorylation, propagation, truncation, ubiquitin.

Correspondence: Tetsuaki Arai, Associate Professor, Department of Neuropsychiatry, Division of Clinical Medicine, Faculty of Medicine, University of Tsukuba, 1-1-1 Tennoudai, Tsukuba, Ibaraki 305-8575, Japan. Email: 4632tetsu@md.tsukuba.ac.jp

Received 16 February 2014; and accepted 14 May 2014.

HISTORY AND BACKGROUND

Trans-activation response (TAR) DNA-binding protein of M_r 43 kDa (TDP-43) is a major component of the tau-negative and ubiquitin-positive inclusions that characterize amyotrophic lateral sclerosis (ALS) and the most common pathological subtype of frontotemporal lobar degeneration (FTLD-U), which is now referred to as FTLD-TDP.[1–7] Several genes, including the *granulin* (*GRN*),[8,9] *valosin-containing protein* (*VCP*),[10] *TARDBP*[11–15] and *C9ORF72*,[16,17] have been reported to be associated with familial forms of FTLD-TDP and ALS. These disorders are now collectively referred to as TDP-43 proteinopathy.[1–4]

TDP-43 was first isolated as a transcriptional inactivator binding to the TAR DNA element of the HIV-1 virus.[18] It belongs to the group of 2 RNA-binding domain (RBD)-Gly RNA-binding proteins, which include the heterogeneous nuclear ribonucleoprotein (hnRNP) family and factors involved in RNA splicing and transport.[19]

It is known to be involved in multiple cellular processes, including gene transcription, alternative splicing and stabilization of mRNA, microRNA biogenesis, apoptosis, and cell division.[20–28]

Ubiquitin- and TDP-43-positive pathological inclusions found in FTLD-TDP include neuronal cytoplasmic inclusions (NCIs), dystrophic neurites (DNs), neuronal intranuclear inclusions (NIIs), and glial cytoplasmic inclusions (GCIs).[1,2,29–31] In ALS, motoneuronal skein-like inclusions (SLIs) immunopositive for ubiquitin had been regarded as one of the major pathological hallmarks.[32–34] Recent detailed immunohistochemical studies have clarified the wide distribution of neuronal and glial TDP-43 pathology in multiple areas of the CNS, including nigrostriatal system, the neocortical and allocortical areas, and the cerebellum.[35,36] These findings suggest that ALS does not selectively affect only the motor system, but rather is a

multisystem neurodegenerative TDP-43 proteinopathy affecting both neurons and glial cells.[35,36]

Biochemical analyses of the detergent-insoluble fraction extracted from brains of patients afflicted with FTLD-TDP and ALS show that TDP-43 accumulated in these pathological structures is phosphorylated, proteolytically cleaved and ubiquitinated.[1,2]

In the present review, we will focus on significance and limitation of the pathological classification of TDP-43 proteinopathy, based on the immunohistochemical and biochemical examinations of diseased brains.

DEFINITION AND DIFFERENTIALS

Definition of TDP-43 positive structures

NCIs (Fig. 1A,B)

The appearance of ubiquitin-positive tau-negative NCIs in the hippocampal region was first recognized in patients with ALS,[37] and was subsequently found in those with FTLD with motor neuron disease (FTLD-MND)[38,39] and in FTLD without MND.[40–42] TDP-43 positive NCIs are frequently found in the frontotemporal neocortex and the dentate granule cells of the hippocampus. Characteristically, by immunohistochemistry using phosphorylation-independent anti-TDP-43 antibodies, normal nuclear staining of TDP-43 is lost in neurons with NCIs.[1,3]

NIIs (Fig. 1B)

Ubiquitin-positive NIIs in FTLD-U were first reported in familial cases.[43,44] They have a lentiform or "cat's eye" appearance and are present in small neurons in multiple neuroanatomical sites. They are observed more frequently in familial cases than in sporadic cases.[35]

DNs (Fig. 1C)

Two types of DNs, short DNs and elongated DNs, are recognized.[45,46] They are positive for both TDP-43 and ubiquitin. Both types of DNs are typically most numerous in layer II of the frontal and temporal cortices, although the

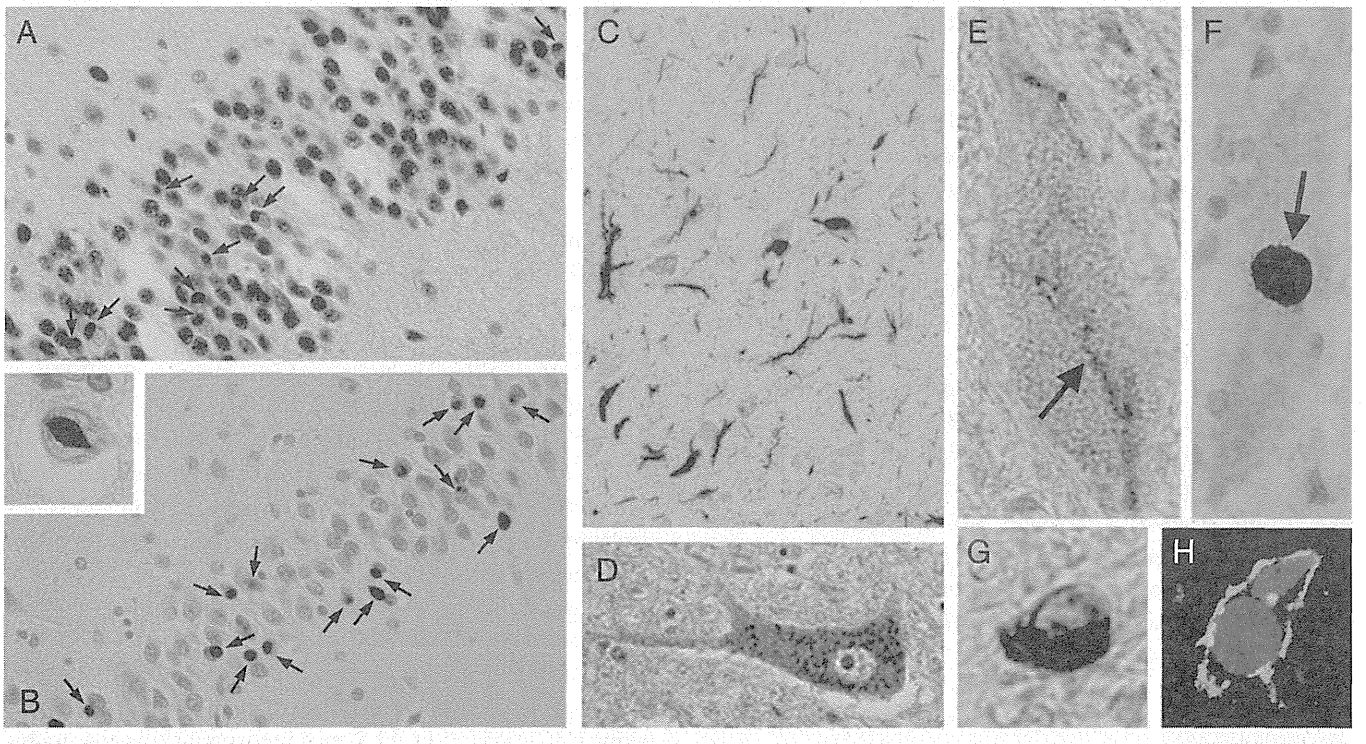

Fig. 1 Neuronal and glial structures immunopositive for trans-activation response (TAR) DNA-binding protein of M_r 43 kDa (TDP-43) in frontotemporal lobar degeneration with TDP-43 pathology (FTLD-TDP) and amyotrophic lateral sclerosis (ALS) A. Dentate gyrus (DG) of the hippocampus of the FTLD-TDP case stained with the commercially available phosphorylation-independent anti-TDP-43 antibody. Both neuronal cytoplasmic inclusions (NCIs) (arrows) and normal neuronal nuclei are immunopositive. B. DG of the FTLD-TDP case stained with the phosphorylated TDP-43-specific antibody (pS409/410). NCIs (arrows) are stained with no nuclear staining. Inset reveals a neuronal intranuclear inclusion with a "cat's eye" shape. C. Dystrophic neurites (DNs) in the frontal cortex of the FTLD-TDP positive for pS409/410. Cytoplasmic granular structures ("preinclusion") stained with the phosphorylation-independent anti-TDP-43 antibody (D), and skein-like inclusion (E), round inclusion (F), and glial cytoplasmic inclusion (G) stained with pS409/410 in the anterior horn of the ALS cases. In double-label immunofluorescence histochemistry using pS409/410 (red in H) and anti-C4d (green in H), the pS409/410-positive inclusion (red) is present around the nucleus of the C4d-positive oligodendrocyte (green).

elongated DNs are generally more widely dispersed throughout the entire cortex compared with the short DNs.[46] Such morphological features of DNs are one of the factors to determine the pathological classification of FTLD-TDP as described below.

Preinclusions (Fig. 1D)

Diffuse or granular cytoplasmic staining of TDP-43 are frequently found in motor neurons of cranial nerve nuclei or spinal cord of ALS and FTLD-TDP cases. They are sometimes referred as preinclusions, and are thought to show a transitional stage in which cytoplasmic TDP-43 remains unassembled or partially assembled into inclusions.[3,35] Mori *et al.* newly found two types of TDP-43 positive neuronal cytoplasmic structures in ALS cases, linear wisps and dot-like inclusions, which may be premature structures of SLIs and round inclusions (RIs), respectively.[47]

SLIs (Fig. 1E) and round inclusions (Fig. 1F)

The SLIs were first reported by Leigh *et al.* as a ubiquitin-positive, skein-like array in anterior horn cells in MND.[32,33] SLIs and spherical or round inclusions in the motoneurons are specific for sporadic ALS cases and found in 100% of them.[34]

GCIs (Fig. 1G,H)

GCIs are immunopositive for TDP-43[1,2,35] (Fig. 1G) and p62,[48] but are mostly negative for ubiquitin.[35,48] In double immunofluorescence staining forphosphorylated TDP-43 (pTDP-43) and a complement protein, C4d, pTDP-43 positive inclusions are often found in C4d-positive oligodendrocytes (Fig. 1H), indicating that most GCIs are of oligodendrocytic origin.[49] They are more frequent in the white as compared with the gray matter.[35] They are found in most cases of TDP-43 proteinopathy to varying degrees, but are the most frequent in ALS and FTLD-MND cases.

Classification of TDP-43 pathology in TDP-43 proteinopathy

Based on cerebral ubiquitin immunohistochemistry, FTLD-TDP was classified into three subtypes by Sampathu *et al.*[31] and Mackenzie *et al.*.[29] Unfortunately, the numbering schemes used in these two systems do not match. Then, Cairns *et al.* drew these two systems together into a unified scheme, and added familial FTLD-TDP with *VCP* mutations.[45] Finally, in 2011, the classification systems were harmonized,[50] and four subtypes were recognized (Fig. 2A): type A had numerous NCIs and short DNs; type B had numerous NCIs with few DNs; type C was characterized by DNs which were often longer and thicker than

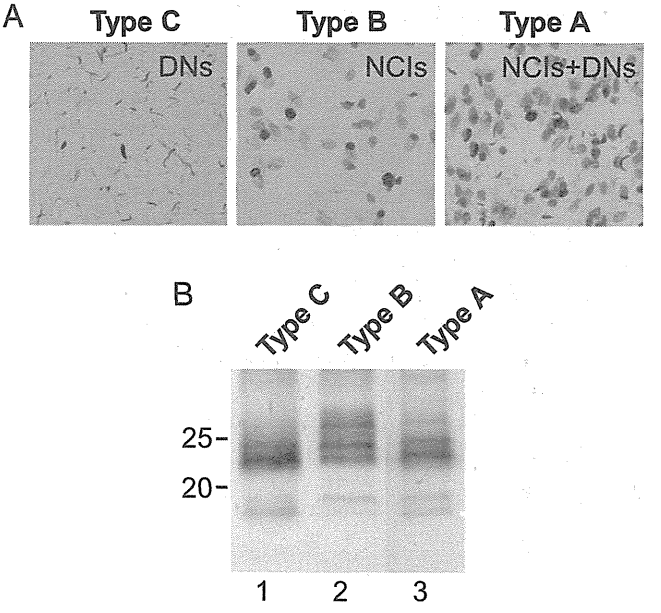

Fig. 2 Pathological and biochemical classification of frontotemporal lobar degeneration with trans-activation response (TAR) DNA-binding protein of M_r 43 kDa (FTLD-TDP). A. FTLD-TDP subtypes A to C. Type A has numerous neuronal cytoplasmic inclusions (NCIs) and short dystrophic neurites (DNs); type B has numerous NCIs; type C is characterized by long and tortuous DNs. B. Representative immunoblots with the phosphorylated TDP-43 specific antibody, pS409/410. The sporadic FTLD-TDP case with type C pathology shows two major bands at 23 and 24 kDa and two minor bands at 18 and 19 kDa (lane 1), while the FTLD-MND (motor neurone disease) case with type B pathology shows three major bands at 23, 24 and 26 kDa and two minor bands at 18 and 19 kDa (lane 2). A 23 kDa band is the most intense in sporadic FTLD-TDP (lane 1), while a 24 kDa band is the most intense in FTLD-MND (lane 2). The band pattern of the case of familial FTLD with *GRN* gene mutation with type A pathology is not distinctive but intermediate between FTLD-TDP and FTLD-MND (lane 3).

DNs in type A, with few NCIs; and type D had numerous NIIs and DNs with few NCIs.

Josephs *et al.* reported the proportion of subtypes based on pooled data from four large clinicopathological studies: the most common subtype was type A accounting for 41% of FTLD-TDP cases, followed by type B with 34% and then type C with 25%.[51] In 29 cases of FTLD-TDP collected in the Tokyo Metropolitan Institute of Medical Science, the proportion of cases showing types A, B and C was 17%, 48% and 34%, respectively.[52] The lower frequency of type A in our series may be partly explained by the low frequency of familial cases of FTLD in Japan.[52–54]

ALS is pathologically classified into two types based on the TDP-43 neuronal distribution pattern by Nishihira *et al.*[36] Type 2 is distinguished from type 1 by the TDP-43-positive NCIs in the frontotemporal cortex, hippocampal formation, neostriatum and substantia nigra, and is significantly associated with dementia.

Association between clinical and pathological subtypes of TDP-43 proteinopathy

FTLD is clinically subclassified into three categories: behavioral variant frontotemporal dementia (bvFTD), semantic dementia (SD) and progressive non-fluent aphasia (PNFA). The strong correlations between the subtype of TDP-43 pathology and clinical phenotype are indicated, although a strict one-to-one relationship is lacking.[55] Type C is associated with SD, type B with FTLD with motor neuron disease (MND) or clinical sign of MND, and type A with PNFA.[29,51,52,56,57] bvFTD is not as strongly associated with any one type.[51,52,56] As for the correlation between genetics and subtypes, *GRN* mutations are associated with type A, *C9OFR72* with types A and B, and *VCP* with type D.

UNDERLYING MECHANISM

Phosphorylation and truncation of TDP-43 accumulated in diseased brains

There are multiple potential phosphorylation sites within human TDP-43, including 41 serine (Ser), 15 threonine (Thr) and seven tyrosine (Tyr) residues. In order to identify the critical phosphorylation sites of TDP-43 accumulated in diseased brains, we raised antibodies against 39 different synthetic phosphopeptides, representing 36 out of 63 candidate phosphorylation sites.[58] The major strategy was to choose Ser and Thr residues that cover known protein kinase consensus phosphorylation motifs, including R-X-pSer/Thr for protein kinase A (PKA), pSer/Thr-X-X-Ser/Thr for CK1, pSer/Thr-X-X-E/D for CK2, pSer/Thr-X-X-X-Ser for GSK3 and CK1. Additionally, Ser/Thr residues in the C-terminal region of TDP-43 were chosen because they are analogous to abnormal phosphorylation sites found in tau or α-synuclein.

Of the generated antibodies, pS379, pS403/404, pS409, pS410 and pS409/410 stained the inclusions in immunohistochemistry, and abnormal TDP-43 species on immunoblot, in FTLD-TDP and ALS cases. These results suggest that at least five sites on TDP-43 are phosphorylated in subjects with FTLD-TDP and ALS, and that abnormal phosphorylation takes place mainly near the C-terminal region of TDP-43. This is similar to tauopathies and synucleinopathies, where multiple Ser residues in the C-terminal region in tau and Ser129 in α-synuclein, are abnormally phosphorylated.[59,60] Phosphorylation of Ser409/410 of TDP-43 accumulated in diseased brains was confirmed by other groups.[61,62]

In contrast to the commercially obtained phosphorylation-independent anti-TDP-43 antibody, which labels both abnormal structures and normal nuclei (Fig. 1A), pTDP-43 specific antibodies recognize only abnormal structures, including NCIs (Fig. 1B), NIIs (Fig. 1B, inset), DNs (Fig. 1C), SLIs (Fig. 1E), round inclusions (Fig. 1F) and GCIs (Fig. 1G,H). These results suggest that all of the inclusion types previously described in FTLD-TDP and ALS contain pTDP-43.

Immunoblot analyses of sarkosyl-insoluble fractions with pTDP-43-specific antibodies reveal a single band at 45 kDa, several smaller fragments at ~25 kDa and indistinct smears in FTLD-TDP and ALS cases but not in controls. The intensity of the ~25 kDa fragments tends to be greater than that of the 45 kDa band in FTLD-TDP and in ALS.

Biochemical features of pathological subtypes of FTLD-TDP

To investigate the biochemical basis of the different TDP-43 pathological subtypes (type A-C), we carefully compared the results of immunoblots of the sarkosyl-insoluble fractions from the cerebral cortex of cases with sporadic FTLD-TDP (type C), FTLD-MND (type B), ALS (type B) and familial FTLD with *GRN* mutations (type A), using pTDP-43-specific antibodies. The results showed that there is a close relationship between the pathological subtypes and the immunoblot pattern of the 18~26 kDa C-terminal fragments of pTDP-43[58] (Fig. 2). These results parallel our earlier findings of differing C-terminal tau fragments in progressive supranuclear palsy (PSP) and corticobasal degeneration (CBD), despite identical composition of tau isoforms.[63]

Prion-like properties of pathological TDP-43

Prion-like propagation of aggregated proteins in neurodegenerative diseases has been well established.[64–73] In prion diseases, the banding patterns of protease-resistant prion protein extracted from diseased brains have been reported to differ among the subtypes.[74] For instance, protease-resistant prion protein extracted from cases with new-variant Creutzfeldt–Jakob disease showed a different and characteristic pattern from that in cases with sporadic Creutzfeldt–Jakob disease. Protease-treated prion protein species are thought to have different mobilities because of different conformations. These findings in prion disease suggest that the different band patterns in TDP-43 proteinopathies may represent different conformations of abnormal TDP-43 in the diseases. Indeed, Tsuji *et al.* found that on chymotrypsin treatment of Sarkosyl-insoluble pellets extracted from brains of patients with FTLD-TDP, the patterns of multiple protease-resistant bands of TDP-43 at 16–25 kDa differed among three subtypes of FTLD-TDP.[75] In addition, there is no difference between the band pattern of TDP-43 C-terminal fragments in cortex

Table 1 Comparison between FTLD-PLS and FTLD-ALS[52]

	FTLD-PLS	FTLD-ALS
Clinical features		
LMN signs	Absent	Present
UMN signs	Present	Present
Pathological features		
CST degeneration	Severe	Mild
LMN loss	Absent (or minimal)	Evident
TDP-43 positive NCIs in LMN	Absent (or rare)	Present
TDP-43 positive RSs in the neuropil of SC	Present	Absent
Bunina bodies	Absent	Present
Common subtype of TDP-43 pathology	Type C	Type B

CST, corticospinal tract; FTLD-ALS, frontotemporal lobar degeneration with amyotrophic lateral sclerosis; FTLD-PLS, frontotemporal lobar degeneration with primary lateral sclerosis; LMN, lower motor neuron; NCIs, neuronal cytoplasmic inclusions; RSs, round structures; SC, spinal cord; UMN, upper motor neuron.

and that in spinal cord in ALS cases, suggesting that abnormal proteins produced in cells is transferred to different regions and propagated.[75,76]

Furthermore, using the cell culture system, Nonaka *et al.* showed that insoluble TDP-43 aggregates in brains of ALS and FTLD-TDP patients have prion-like properties. They showed that insoluble TDP-43 extracted from brains of each subtype of FTLD-TDP (types A, B or C) cases functioned as seeds for TDP-43 aggregation in cultured cells.[77] Interestingly, the band patterns of TDP-43 C-terminal fragments in the insoluble fraction of cells expressing TDP-43 in the presence of each type of seed were different from each other, but quite similar to that of insoluble TDP-43 prepared as seeds from the corresponding patients. These results suggest that seed-dependent TDP-43 aggregation occurs in a self-templating manner like prion aggregation. They also showed prion-like properties of abnormal TDP-43, including stability to heat and proteinases, and cell-to-cell transmission at least partly via exosomes.[77]

CURRENT AMBIGUITIES AND PERSPECTIVE

FTLD-PLS

Recently, the presence of FTLD-TDP showing corticospinal tract (CST) degeneration but lacking lower motor neuron (LMN) loss was reported[78–80] and the term primary lateral sclerosis (PLS) is used to distinguish MND of these cases from ALS.[78,79] Of 29 FTLD-TDP cases collected in Tokyo Metropolitan Institute of Medical Science, we identified 10 FTLD with PLS (FTLD-PLS) cases.[52]

Clinically, the first symptoms were bvFTD in five cases, SD in three cases and PNFA in one case. The upper motor neuron (UMN) signs, including hyperreflexia, spasticity, Babinski's sign, paralysis and ankle clonus, were recorded in six cases, and five of six cases developed UMN signs in the middle or late stage of the disease. There were no LMN signs in any case. In terms of the TDP-43 pathology, six cases showed type C, three cases type A, and one case type B. In four cases in which the spinal cord was available, there were no skein-like inclusions or round inclusions in all cases, but TDP-43 positive round structures in the neuropil of the anterior horn were found in two cases with type C TDP-43 pathology. The clinicopathological comparison between FTLD-PLS and FTLD-ALS is summarized in Table 1. These results suggest that FTLD-PLS may be a significant clinicopathological entity distinct from FTLD-ALS.[52] The different band pattern of C-terminal fragments of TDP-43 on immunoblotting of sarkosyl-insoluble fraction between FTLD-PLS and ALS, reported by Kosaka *et al.*,[81] further supports our notion. Recently, Josephs *et al.* reported that of three subtypes of FTLD, CST was associated mostly with FTLD with type C pathology with predominant atrophy of the right temporal lobe.[82]

The significance of TDP-43 pathology in other neurodegenerative disorders

Immunohistochemical examination, using commercially available phosphorylation-independent anti-TDP-43 antibodies, had demonstrated abnormal intracellular accumulation of TDP-43 in neurodegenerative disorders other than FTLD-TDP and ALS, including ALS/parkinsonism-dementia complex of Guam,[83–85] Alzheimer's disease (AD),[86–90] dementia with Lewy bodies (DLB),[87,91] Pick's disease,[2,92,93] hippocampal sclerosis,[86] CBD[90] and PSP.[94] By immunohistochemical and biochemical analyses using pTDP-43-specific antibodies, we found a high frequency of pTDP-43 pathology in cases of AD (36–56%) (Fig. 3A,C), DLB (53–60%) (Fig. 3B,D), argyrophilic grain disease (AGD) (60%) (Fig. 3E), Huntington's disease (100%) and a case of familial British dementia.[95–98]

The pathological significance and mechanism of such frequent co-occurrence of diverse protein aggregates are